CHANNELS
2019, VOL. 13, NO. 1, 440–454
https://doi.org/10.1080/19336950.2019.1676368

Taylor & Francis
Taylor & Francis Group

RESEARCH PAPER

OPEN ACCESS Check for updates

Anterograde trafficking signals in $GABA_A$ subunits are required for functional expression

Jessica L. Nuwer and Mark W. Fleck

Neuroscience & Experimental Therapeutics, Albany Medical College, Albany, NY, USA

ABSTRACT

Pentameric $GABA_A$ receptors are composed from 19 possible subunits. The $GABA_A$ β subunit is unique because the β_1 and β_3 subunits can assemble and traffic to the cell surface as homomers, whereas most of the other subunits, including β_2, are heteromers. The intracellular domain (ICD) of the $GABA_A$ subunits has been implicated in targeting and clustering $GABA_A$ receptors at the plasma membrane. Here, we sought to test whether and how the ICD is involved in functional expression of the β_3 subunit. Since θ is the most homologous to β but does not form homomers, we created two reciprocal chimeric subunits, swapping the ICD between the β_3 and θ subunits, and expressed them in HEK293 cells. Surface expression was detected with immunofluorescence and functional expression was quantified using whole-cell patch-clamp recording with fast perfusion. Results indicate that, unlike β_3, neither the β_3/θ_{IC} nor the θ/β_{3IC} chimera can traffic to the plasma membrane when expressed alone; however, when expressed in combination with either wild-type α_3 or β_3, the β_3/θ_{IC} chimera was functionally expressed. This suggests that the ICD of α_3 and β_3 each contain essential anterograde trafficking signals that are required to overcome ER retention of assembled $GABA_A$ homo- or heteropentamers.

ARTICLE HISTORY
Received 2 July 2019
Revised 16 September 2019
Accepted 25 September 2019

KEYWORDS
GABAA; trafficking; beta subunit; theta subunit; chimera

Introduction

Epilepsy, anxiety, neurodevelopmental disorders, and neuropsychiatric disorders collectively affect a significant proportion of the population. One common problem in these disorders is the dysfunction of the $GABA_A$ receptor, so it is important to understand how these receptors are functionally regulated. $GABA_A$ receptors are the target of anesthetics as well as drugs that are used as anticonvulsives, anxiolytics, and hypnotics [1]. They are pentameric ligand-gated chloride channels in the Cys-Loop superfamily of ligand-gated ion channels. Their role is to mediate fast inhibitory neuronal transmission. The pentameric ion channel is formed from a pool of 19 different $GABA_A$ subunits ($\alpha_{1\text{-}6}$, $\beta_{1\text{-}3}$, $\gamma_{1\text{-}3}$, δ, ε, θ, π, and $\rho_{1\text{-}3}$) [1], with each subunit having the same general structure: a long N-terminal domain (NTD) which creates the extracellular ligand binding domain (LBD), 4 transmembrane domains (TMD) that create the ion channel pore, a variable length intracellular domain (ICD) composed of the TM3-TM4 loop, and a short extracellular C-terminus (CTD) [1,2]. Considering the vast number of possible subunit combinations that could exist, it is important to understand the cellular mechanisms that limit the functional expression (assembly and trafficking) of subunit combinations that might otherwise exist. Most of the known combinations require α and β subunits; however, the rules that govern assembly and regulate trafficking of the receptors are still poorly understood.

Canonical $GABA_A$ receptors contain 2 α subunits, 2 β subunits, and a third X subunit arranged counterclockwise around the central pore in the order: β-α-β-α-X; where X is typically a γ subunit; however, it is generally accepted that α, β, δ, or one of the other subunits can replace the γ [1]. Some of the structural elements that are involved in regulated assembly of compatible subunits have been identified, most commonly in the NTD binding loops that form the subunit-subunit interface [3–7]. Assembly of the β subunit is unique in that the β_1 and β_3 subunits can assemble and traffic to the plasma membrane as homomeric receptors, whereas most of the other subunits, including β_2, are obligatory heteromers [8]. β_1, β_2 and β_3 are at

CONTACT Mark W. Fleck fleckm@amc.edu

minimum 70% homologous but show differences in homomeric assembly. The critical determinant of β_3 homomeric functional expression was identified as the so-called GKER sequence, located in the extracellular domain (ECD) binding loop F of β_3, which corresponds to a DNTK sequence at the equivalent site in β_2[7]. Using chimeric exchanges between β_2 and β_3, Taylor et. al. (1999) [7] showed that the GKER sequence was necessary for β_3 and sufficient to rescue β_2. This study implied that the determinants of functional expression are entirely contained in the NTD; however, there may be other determinants of functional expression that were not revealed in that study because they are sufficiently conserved across the β subunits. The TM3-TM4 intracellular loop (intracellular domain, ICD) has been implicated in targeting, anchoring, and clustering of the $GABA_A$ receptor at the plasma membrane; however, the mechanism of how this loop is involved in $GABA_A$ receptor functional expression is still largely unknown.

Here, we sought to test whether and how the ICD is involved in functional expression of the β_3 subunit. We created two reciprocal chimeric subunits, one having the EC and TM domains from β_3 and the ICD from θ, and the other having the EC and TM domains from θ and the ICD from β_3. The θ subunit was chosen as the chimeric donor because it is most homologous to β but forms heteromeric and not homomeric receptors [9]. Moreover, the θ ICD shares virtually no homology with the β_3 ICD or any other subunit. Because there is no evidence for ICD involvement in assembly, we hypothesized that the θ ICD would support the functional expression of β_3 as either homomers or heteromers. We used immunofluorescence staining to test plasma membrane expression and whole-cell patch-clamp with fast perfusion to test receptor function.

Results indicate that neither the β_3/θ_{IC} nor the θ/β_{3IC} chimera can traffic to the plasma membrane when expressed alone, suggesting the β_3 ICD is necessary for functional homomeric expression but is insufficient to traffic unassembled θ subunits to the plasma membrane. When expressed in combination with either wild-type α_3 or β_3, the β_3/θ_{IC} chimera was rescued to the plasma membrane and the receptor functioned essentially like the wild type β-containing receptor, while the θ/β_{3IC} chimera was not rescued. This suggests that the TM3-TM4 intracellular loops of α_3 and β_3 each contain essential anterograde trafficking signals that are required to overcome ER retention of assembled homo- or heteropentamers.

Results

The IC loop of θ disrupts β_3 homomeric plasma membrane expression

To determine how the intracellular loop is involved in functional expression, we produced a reciprocal pair of chimeric receptors (β_3/θ_{IC} and θ/β_{3IC}) swapping the β_3 and θ ICDs Figure 1(a). Unlike β_3, θ subunits do not assemble or express as homomeric receptors on the plasma membrane [9]. To visualize expression, the wild-type β_3 and both chimeric constructs were tagged with three consecutive hemagglutinin epitopes (HA) on the N-terminus between amino acids 5 and 6 ($^{HA}\theta/\beta_{3IC}$) or 6 and 7 ($^{HA}\beta_3$, $^{HA}\beta_3/\theta_{IC}$) of the mature protein. Western blotting analysis was performed to confirm that the chimeric constructs are full length and expressed with a similar relative abundance compared to either the $^{HA}\beta_3$ or the $^{HA}\theta$ construct. As expected, $^{HA}\beta_3/\theta_{IC}$ was found to be a similar molecular weight as $^{HA}\theta$ ($^{HA}\beta_3/\theta_{IC}$ calculated MW = 74 kDa, actual MW = 91 kDa and $^{HA}\theta$ calculated MW = 77 kDa, actual MW = 95 kDa). Likewise, $^{HA}\theta/\beta_{3IC}$ was found to be a similar molecular weight as $^{HA}\beta_3$ ($^{HA}\theta/\beta_{3IC}$ calculated MW = 61 kDa, actual MW = 63 kDa and $^{HA}\beta_3$ calculated MW = 58 kDa, actual MW = 64 kDa). GAPDH was used as a loading control and had a molecular weight of 36 kDa, as expected. Relative to GAPDH, the expression ratio of $^{HA}\beta_3$ was 1.87, $^{HA}\theta$ was 1.36, $^{HA}\beta_3/\theta_{IC}$ was 1.53, and $^{HA}\theta/\beta_{3IC}$ was 1.61 Figure 1(b). Next, we used immunofluorescence to visualize and quantify subunit expression in non-permeabilized cells (surface) and after Triton-X permeabilization (total). When expressed alone in HEK293 cells, $^{HA}\beta_3$ was clearly labeled on the surface of many cells, as shown by non-permeabilized staining with an anti-HA antibody Figure 1(c,d). In contrast, $^{HA}\beta_3/\theta_{IC}$ was rarely found on the surface (max 1–5 cells per dish compared to ≥ 150 cells for $^{HA}\beta_3$); but, when it was seen, the fluorescence intensity was comparable to $^{HA}\beta_3$ ($^{HA}\beta_3/\theta_{IC}$ = 14.3 ± 2.8 AU, n = 10 images (10 cells)

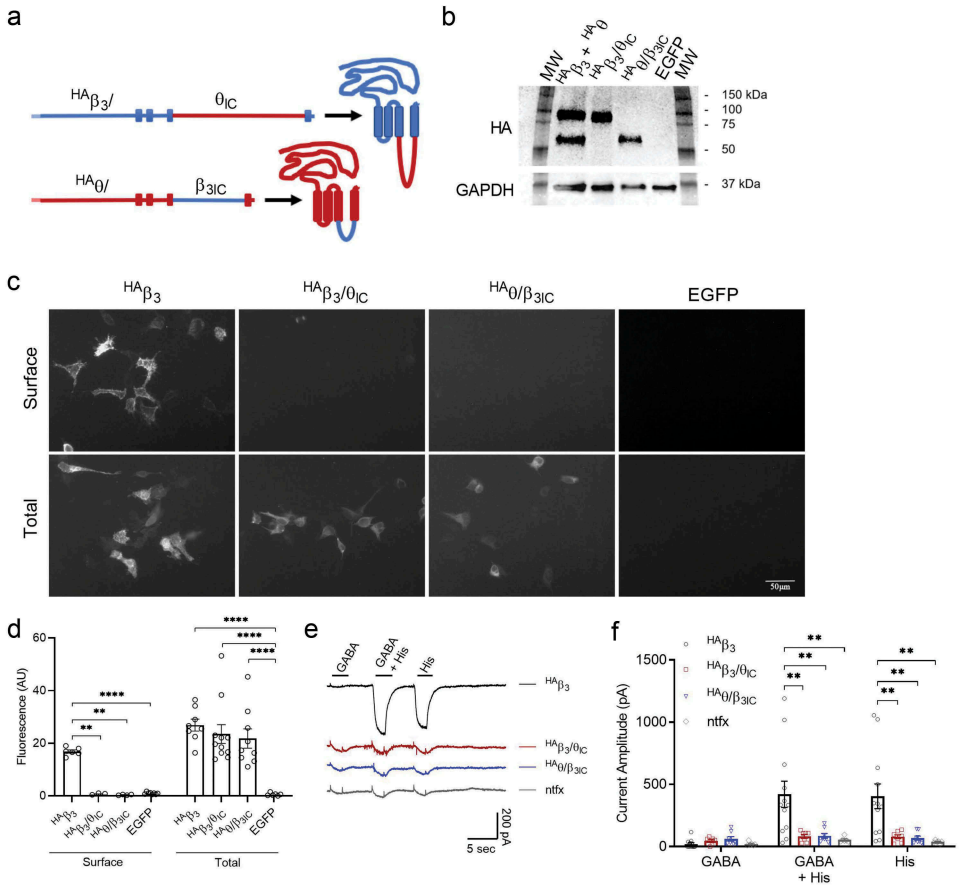

Figure 1. Homomeric expression and function of β_3 and chimera.
a) Schematic of the $^{HA}\beta_3/\theta_{IC}$ and $^{HA}\theta/\beta_{3IC}$ chimeras where the blue portions are from β_3 and the red portions are from θ. b) Total protein Western blot of $^{HA}\beta_3$ + $^{HA}\theta$, $^{HA}\beta_3/\theta_{IC}$, $^{HA}\theta/\beta_{3IC}$, and EGFP transfected HEK293 cells. The membrane was probed with primary rabbit anti-HA Epitope Tag (1:5000 dilution) and rabbit anti-GAPDH (1:5000 dilution) and secondary goat anti-rabbit-HRP (1:5000 dilution). HA bands were quantified as fold-changes against GAPDH using ImageJ. Compared to GAPDH, the ratio of $^{HA}\beta_3$ = 1.87; $^{HA}\theta$ = 1.36; $^{HA}\beta_3/\theta_{IC}$ = 1.53; $^{HA}\theta/\beta_{3IC}$ = 1.61. c) Representative IF images at 20x magnification of non-permeabilized (surface) and permeabilized (total) staining of $^{HA}\beta_3$, $^{HA}\beta_3/\theta_{IC}$, $^{HA}\theta/\beta_{3IC}$, or EGFP expressed alone in HEK293 cells. Expression was determined using a rabbit anti-HA Epitope Tag DyLight™ 549 conjugated antibody at 1:1000 dilution. d) Bar graphs portray the mean ± SEM of Fiji ImageJ fluorescence quantification of $^{HA}\beta_3$ (n_{surf} = 6 images (46 cells), n_{total} = 8 images (79 cells)); $^{HA}\beta_3/\theta_{IC}$ (n_{surf} = 4 images (0 cells), n_{total} = 11 images (97 cells)); and $^{HA}\theta/\beta_{3IC}$ (n_{surf} = 4 images (0 cells), n_{total} = 9 images (31 cells)) IF images from c with individual data points overlaid. e) Representative traces of $^{HA}\beta_3$ (n = 12), $^{HA}\beta_3/\theta_{IC}$ (n = 7/8), and $^{HA}\theta/\beta_{3IC}$ (n = 8/10) in response to 1 mM GABA and 3 mM histamine applied separately or together. f) Bar graphs portray the mean ± SEM of peak current amplitudes from whole-cell recordings in e with individual data points overlaid. * = $p < 0.05$; ** = $p < 0.01$; *** = $p < 0.001$; **** = $p < 0.0001$; using 2-way ANOVAs with Bonferroni post hoc comparisons.

and $^{HA}\beta_3$ = 16.9 ± 0.6 AU, n = 6 images (46 cells)). $^{HA}\theta/\beta_{3IC}$ was never found to be labeled on the surface of cells (n = 4 images (0 cells)). Total expression levels of the $^{HA}\beta_3$, $^{HA}\beta_3/\theta_{IC}$, and $^{HA}\theta/\beta_{3IC}$ constructs were comparable in terms staining intensity and cell number with the exception of $^{HA}\theta/\beta_{3IC}$, which showed fewer cells labeled ($^{HA}\beta_3$ = 26.9 ± 2.3 AU, n = 8 images (79 cells); $^{HA}\beta_3/\theta_{IC}$ = 23.5 ± 3.6 AU, n = 11 images (97 cells); and $^{HA}\theta/\beta_{3IC}$ = 21.8 ± 3.7 AU, n = 9 images (31 cells)) when the cells were re-probed following permeabilization.

Functionally, β_3 homomers are gated by histamine and only weakly, if at all, by GABA [10,11]. To better quantify functional expression levels, we used patch clamp recording with fast perfusion to measure whole cell currents in response to 1 mM GABA and 3 mM histamine applied separately or together Figure 1(e,f). As expected, $^{HA}\beta_3$ homomeric receptors exhibited robust responses to both histamine and GABA + histamine in all cells recorded. $^{HA}\beta_3$ homomeric receptors showed large histamine-evoked currents (404 ± 96 pA, n = 12),

which were similar when GABA and histamine were co-applied (420 ± 101 pA, n = 12). GABA-evoked currents were comparatively small (21 ± 10 pA, n = 12) and unreliable. $^{HA}\beta_3/\theta_{IC}$ had one non-responsive cell, resulting in 7 out of 8 recordings with measurable responses. From the responding cells, homomeric $^{HA}\beta_3/\theta_{IC}$ chimeric receptors generated very small currents in response to histamine (70 ± 17 pA, n = 7/8) or GABA + histamine (74 ± 1 pA, n = 7/8), which were significantly smaller than $^{HA}\beta_3$ currents (p = 0.006 and p = 0.003, respectively). $^{HA}\beta_3/\theta_{IC}$ also generated very small GABA-evoked currents (43 ± 10 pA, n = 7/8), however these were not significantly different from $^{HA}\beta_3$ currents (21 ± 10 pA, n = 12, p > 0.9) or currents from non-transfected cells (21 ± 6 pA, n = 6/16, p > 0.9). We also tested the reciprocal IC chimera, $^{HA}\theta/\beta_{3IC}$. In this case, 8 out of 10 recordings had measurable responses. Like $^{HA}\beta_3/\theta_{IC}$, homomeric $^{HA}\theta/\beta_{3IC}$ generated very small currents in response to histamine (68 ± 15 pA, n = 8/10) and GABA + Histamine (86 ± 18 pA, n = 8/10), which were significantly smaller than $^{HA}\beta_3$ (p = 0.002 for both comparisons). The GABA currents generated by $^{HA}\theta/\beta_{3IC}$ (62 ± 17 pA, n = 8/10) were also not significantly different from $^{HA}\beta_3$ or non-transfected cells. Taken together, the immunofluorescence and functional results suggest that the β_3 ICD is required for efficient homomeric surface expression but is not sufficient for surface expression in the absence of assembly.

The α_3 subunit rescues chimeric functional expression

The reduction of β_3 functional expression by the θ ICD raises the question of whether this is caused by an assembly or a trafficking defect. Because heteromeric assembly is more common among $GABA_A$ receptors than homomeric assembly, we wanted to know if the θ ICD would also prevent the functional expression of αβ heteromeric receptors. To test this, we co-transfected the untagged α_3 subunit with $^{HA}\beta_3$, $^{HA}\beta_3/\theta_{IC}$, or $^{HA}\theta/\beta_{3IC}$ in parallel cultures of HEK293 cells. $\alpha_3(^{HA}\beta_3)$ and $\alpha_3(^{HA}\beta_3/\theta_{IC})$ showed clear plasma membrane labeling by anti-HA in non-permeabilized conditions Figure 2(a,b). There were similar numbers of surface-labeled cells and the fluorescence intensity trended toward a decrease in $\alpha_3(^{HA}\beta_3/\theta_{IC})$ compared to $\alpha_3(^{HA}\beta_3)$ (14.0 ± 1.7 AU, n = 20 images (100 cells) and 23.4 ± 3.0 AU, n = 5 images (82 cells), respectively) but failed to reach significance (p = 0.07). $\alpha_3(^{HA}\theta/\beta_{3IC})$ showed no anti-HA surface labeling (n = 4 images (0 cells)). Total HA expression was equivalent in all three conditions when the cells were re-probed following permeabilization ($\alpha_3(^{HA}\beta_3)$ = 26.5 ± 6.2 AU, n = 4 images (60 cells); $\alpha_3(^{HA}\beta_3/\theta_{IC})$ = 26.5 ± 2.8 AU, n = 13 images (121 cells); and $\alpha_3(^{HA}\theta/\beta_{3IC})$ = 23.1 ± 5.4 AU, n = 6 images (17 cells)).

Functionally, $\alpha_3\beta_3$ heteromeric receptors are gated by GABA and not by histamine, but the GABA responses are strongly potentiated by histamine [10]. To better quantify functional expression levels, as before, we used patch clamp recording with fast perfusion to measure whole cell currents in response to 1 mM GABA and 3 mM histamine applied separately or together Figure 2(c,d). $\alpha_3(^{HA}\beta_3)$ had measurable responses in all cells recorded, $\alpha_3(^{HA}\beta_3/\theta_{IC})$ had measurable responses in 19 out of 20 cells recorded, $\alpha_3(^{HA}\theta/\beta_{3IC})$ had measurable responses in 3 out of 9 cells recorded, and the control, α_3-only, had measurable responses in 23 out of 28 cells recorded. Comparing the peak amplitudes of GABA-evoked currents, there was no significant difference between $\alpha_3(^{HA}\beta_3)$ and $\alpha_3(^{HA}\beta_3/\theta_{IC})$ (1266 ± 270 pA, n = 19 and 803 ± 155 pA, n = 19/20, respectively) or between $\alpha_3(^{HA}\theta/\beta_{3IC})$ and α_3-only (7 ± 6 pA, n = 3/9 and 66 ± 22 pA, n = 23/28, respectively). On average, the combined response to GABA + histamine was significantly smaller in both the $\alpha_3(^{HA}\beta_3/\theta_{IC})$ and $\alpha_3(^{HA}\theta/\beta_{3IC})$ heteromeric conditions (1983 ± 363 pA, n = 19/20 and 108 ± 19, n = 3/9, respectively) compared to the $\alpha_3(^{HA}\beta_3)$ heteromers (3483 ± 671 pA, n = 19) ($\alpha_3(^{HA}\beta_3/\theta_{IC})$ p = 0.002 and $\alpha_3(^{HA}\theta/\beta_{3IC})$ p = 0.0001). The GABA + histamine response from $\alpha_3(^{HA}\theta/\beta_{3IC})$ was not significantly different from the response from α_3-only transfection conditions. There was no response to histamine alone in $\alpha_3(^{HA}\beta_3/\theta_{IC})$ (10 ± 6 pA, n = 19/20) or $\alpha_3(^{HA}\theta/\beta_{3IC})$ (32 ± 26 pA, n = 3/9) and a comparatively small response, relative to GABA, in $\alpha_3(^{HA}\beta_3)$ (192 ± 61 pA, n = 19), suggesting a small but measurable population of β_3 homomers in the latter condition. For both $\alpha_3(^{HA}\beta_3)$ and

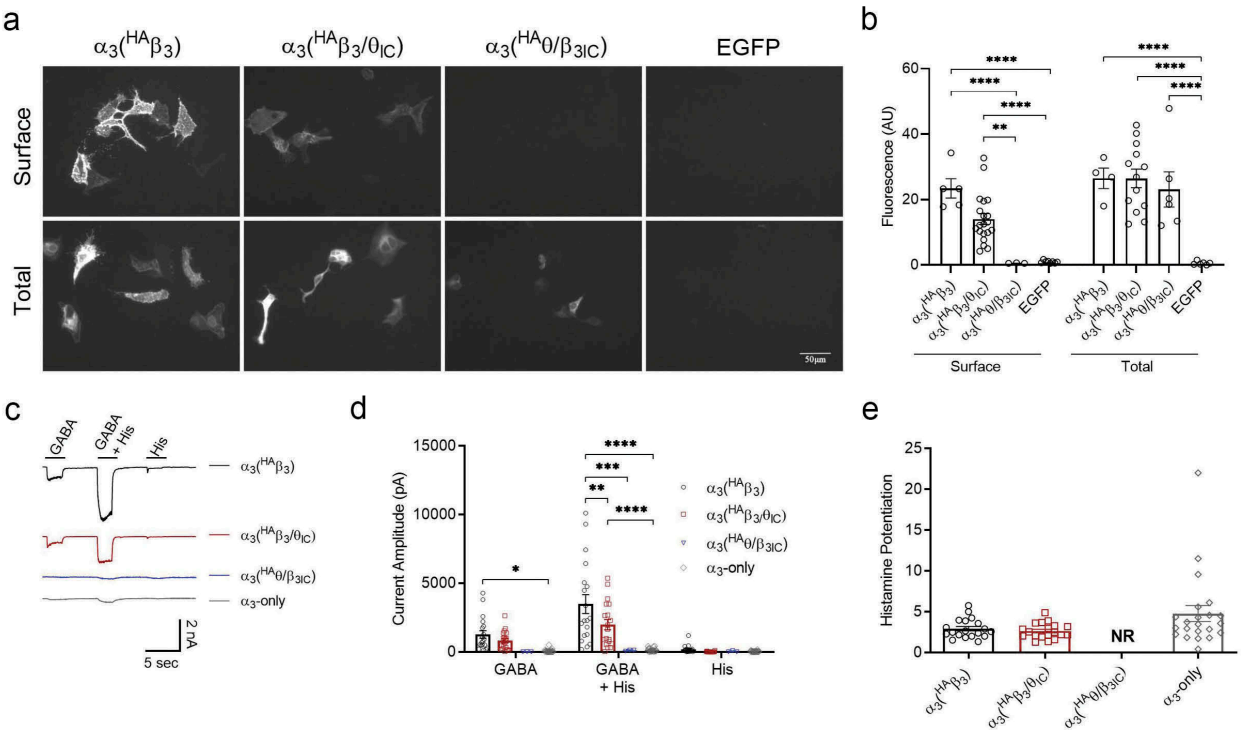

Figure 2. Heteromeric expression and function of β_3 and chimera.
a) IF image at 20x magnification of non-permeabilized (surface) and permeabilized (total) staining of $^{HA}\beta_3$, $^{HA}\beta_3/\theta_{IC}$, or $^{HA}\theta/\beta_{3IC}$ in combination with α_3 co-expressed in HEK293 cells using EGFP as a negative control. Expression was determined using a rabbit anti-HA-549 antibody at 1:1000 dilution. b) Bar graphs portray the mean ± SEM of Fiji ImageJ fluorescence quantification of $\alpha_3(^{HA}\beta_3)$ (n_{surf} = 5 images (82 cells), n_{total} = 4 images (60 cells)); $\alpha_3(^{HA}\beta_3/\theta_{IC})$ (n_{surf} = 20 images (100 cells), n_{total} = 13 images (121 cells)); and $\alpha_3(^{HA}\theta/\beta_{3IC})$ (n_{surf} = 4 images (0 cells), n_{total} = 6 images (17 cells)) IF images from a with individual data points overlaid. c) Representative traces of $\alpha_3(^{HA}\beta_3)$ (n = 19), $\alpha_3(^{HA}\beta_3/\theta_{IC})$ (n = 19/20), and $\alpha_3(^{HA}\theta/\beta_{3IC})$ (n = 3/9) in response to 1 mM GABA and 3 mM histamine applied separately or together. d) Bar graphs portray the mean ± SEM of peak current amplitudes from whole-cell recordings in c with individual data points overlaid. e) Bar graphs portray the mean ± SEM of the degree of histamine potentiation with individual data points overlaid. * = $p < 0.05$; ** = $p < 0.01$; *** = $p < 0.001$; **** = $p < 0.0001$; using 2-way ANOVAs (b and d) or 1-way ANOVAs (e) with Bonferroni post hoc comparisons.

$\alpha_3(^{HA}\beta_3/\theta_{IC})$, the GABA + histamine response was markedly potentiated compared to GABA alone, which is typical of αβ heteromers. There was no difference in the extent of histamine potentiation of the GABA response between $\alpha_3(^{HA}\beta_3)$ (2.93 ± 0.27-fold, n = 19), $\alpha_3(^{HA}\beta_3/\theta_{IC})$ (2.64 ± 0.22-fold, n = 19), and α_3-only (4.78 ± 0.96-fold, n = 22). $\alpha_3(^{HA}\theta/\beta_{3IC})$ only responded to GABA in one recording and thus, could not be included in the statistical analysis. Altogether, these data suggest that the θ ICD chimera functions like the wild-type β_3 subunit, albeit with marginally lower heteromeric surface expression levels and no homomeric surface expression.

To further explore any functional differences caused by the θ ICD, we compared agonist potencies in αβ heteromers containing either $^{HA}\beta_3$ or $^{HA}\beta_3/\theta_{IC}$ (Figure 3). $^{HA}\theta/\beta_{3IC}$ was not included in this experiment due to the lack of response seen in Figure 2. Concentration-response curves were constructed from the peak amplitudes of whole cell currents evoked sequentially by increasing concentrations of GABA (from 1 μM to 1 mM), as shown in Figure 3. Similar to the previous experiment, results showed a trend toward lower maximal peak currents from $\alpha_3(^{HA}\beta_3/\theta_{IC})$ heteromeric receptors (1509 ± 274.6 pA, n = 19) compared to $\alpha_3(^{HA}\beta_3)$ heteromers (2384 ± 258 pA, n = 20); however, this trend failed to reach significance (p = 0.08; Figure 3(a,b). Concentration-response curves were normalized to the maximum GABA concentration tested, and the comparison of these curves revealed a rightward-shift to a 3-fold higher GABA EC_{50} for the chimera-containing heteromer. EC_{50} values were 21 μM (n = 10–20 cells per concentration) for $\alpha_3(^{HA}\beta_3)$

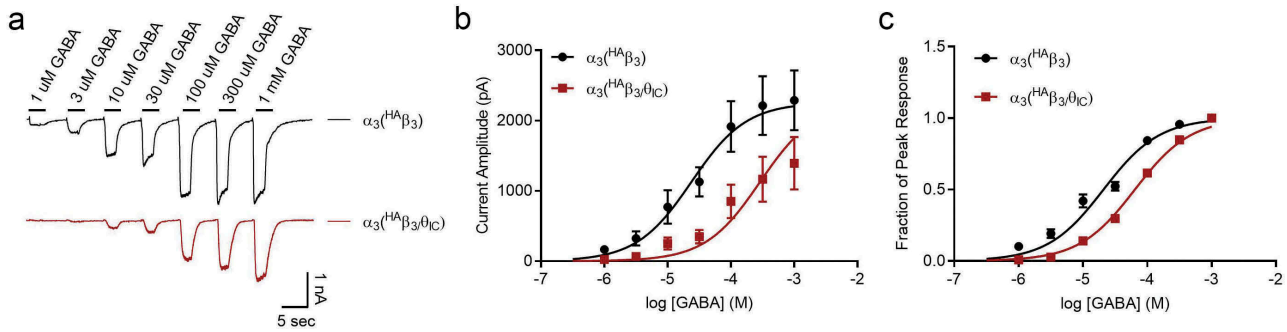

Figure 3. GABA concentration-response curves of αβ heteromeric combinations.
a) Representative traces of GABA-evoked currents from $\alpha_3(^{HA}\beta_3)$ (n = 10–20 cells per concentration) and $\alpha_3(^{HA}\beta_3/\theta_{IC})$ (n = 9–19 cells per concentration) in response to increasing GABA concentrations from 1 μM to 1 mM. b) Raw peak current amplitudes plotted as a function of GABA concentration. Fit parameters: $\alpha_3(^{HA}\beta_3)$ EC_{50} = 28 μM, I_{max} = 2384 pA; $\alpha_3(^{HA}\beta_3/\theta_{IC})$ EC_{50} = 86 μM, I_{max} = 1509 pA. c) Normalized peak amplitudes from B are plotted as a function of GABA concentration. Fit parameters: $\alpha_3(^{HA}\beta_3)$ EC_{50} = 21 μM; $\alpha_3(^{HA}\beta_3/\theta_{IC})$ EC_{50} = 64 μM.

and 64 μM (n = 9–19 cells per concentration) for $\alpha_3(^{HA}\beta_3/\theta_{IC})$ Figure 3(c). It is not clear if the 3-fold potency difference represents an effect of the θ ICD on β_3 subunit function *per se* or a difference in αβ subunit stoichiometry between conditions, which could also explain the trend toward smaller current amplitudes.

The β_3 subunit also rescues chimeric functional expression

Our data clearly show that the $^{HA}\beta_3/\theta_{IC}$ chimera is viable and readily assembles into functional surface-expressed receptors with α_3. Since the known structural determinants for assembly are in the EC ligand binding domains and wild-type β_3 readily assembles in a homomeric configuration, we reasoned that $^{HA}\beta_3/\theta_{IC}$ probably also assembles as homomeric receptors but has a deficit in trafficking introduced by the θ ICD. Such deficit could either result from the loss of an anterograde trafficking signal contained in β ICD or the gain of an ER retention signal in the θ ICD that co-assembly with α_3 can overcome. If so, the next logical question was whether co-assembly with wild-type β_3, having its natural ICD, could also rescue the θ ICD chimera. To test this, we co-transfected the untagged β_3 subunit with $^{HA}\beta_3$, $^{HA}\beta_3/\theta_{IC}$, or $^{HA}\theta/\beta_{3IC}$ in parallel cultures of HEK293 cells to produce pseudo-homomeric β_3 receptors having either the β ICD on all subunits or a mixture of β and θ ICDs. Remarkably, when co-transfected with wild-type β_3, clear surface labeling was seen for both $^{HA}\beta_3$ and $^{HA}\beta_3/\theta_{IC}$, as shown by anti-HA staining in non-permeabilized conditions Figure 4(a,b). Wild-type β_3 co-expression with both $^{HA}\beta_3$ and $^{HA}\beta_3/\theta_{IC}$ yielded comparable numbers of surface-labeled cells with similar intensity ($\beta_3(^{HA}\beta_3)$ = 13.9 ± 0.7 AU, n = 6 images (49 cells) and $\beta_3(^{HA}\beta_3/\theta_{IC})$ = 9.9 ± 1.1 AU, n = 7 images (52 cells)). Co-expression of wild-type β_3 with $^{HA}\theta/\beta_{3IC}$ showed no surface labeling by anti-HA (n = 2 images (0 cells)). When the cells were re-probed following permeabilization there was a significantly higher fluorescence intensity but a similar number of labeled cells in $\beta_3(^{HA}\beta_3/\theta_{IC})$ (25.8 ± 2.6 AU, n = 9 (79 cells)) compared to $\beta_3(^{HA}\beta_3)$ (17.4 ± 1.8 AU, n = 8 (67 cells)) (p = 0.0003). There were not enough fields containing labeled cells for $\beta_3(^{HA}\theta/\beta_{3IC})$ to be included in the statistical analysis (25.0 AU, n = 2 images (7 cells)).

Functionally, we tested the pseudo-homomeric combinations in the same manner as the homomeric receptors and the α_3 heteromers Figure 4(c,d). Since the $\beta_3(^{HA}\beta_3)$ and $\beta_3(^{HA}\beta_3/\theta_{IC})$ combinations both contain the β_3 EC ligand binding and TM domains, the pseudo-homomers were expected to behave like β_3 homomeric receptors and give histamine-evoked but not GABA-evoked currents. Because the $\beta_3(^{HA}\theta/\beta_{3IC})$ combination contains the both the β_3 and θ EC ligand binding domains, and we would not expect the θ NTD to bind histamine, it was unclear how the heteromers should behave if they were produced. The $\beta_3(^{HA}\beta_3)$ and $\beta_3(^{HA}\theta/\beta_{3IC})$ responses were measurable in all cells recorded and the $\beta_3(^{HA}\beta_3/\theta_{IC})$ response was measurable in 13 out of 15 cells. In all conditions, there was a comparable but minimal response to 1 mM GABA ($\beta_3(^{HA}\beta_3)$ = 8 ± 4 pA, n = 14; $\beta_3(^{HA}\beta_3/\theta_{IC})$ = 3 ± 3 pA,

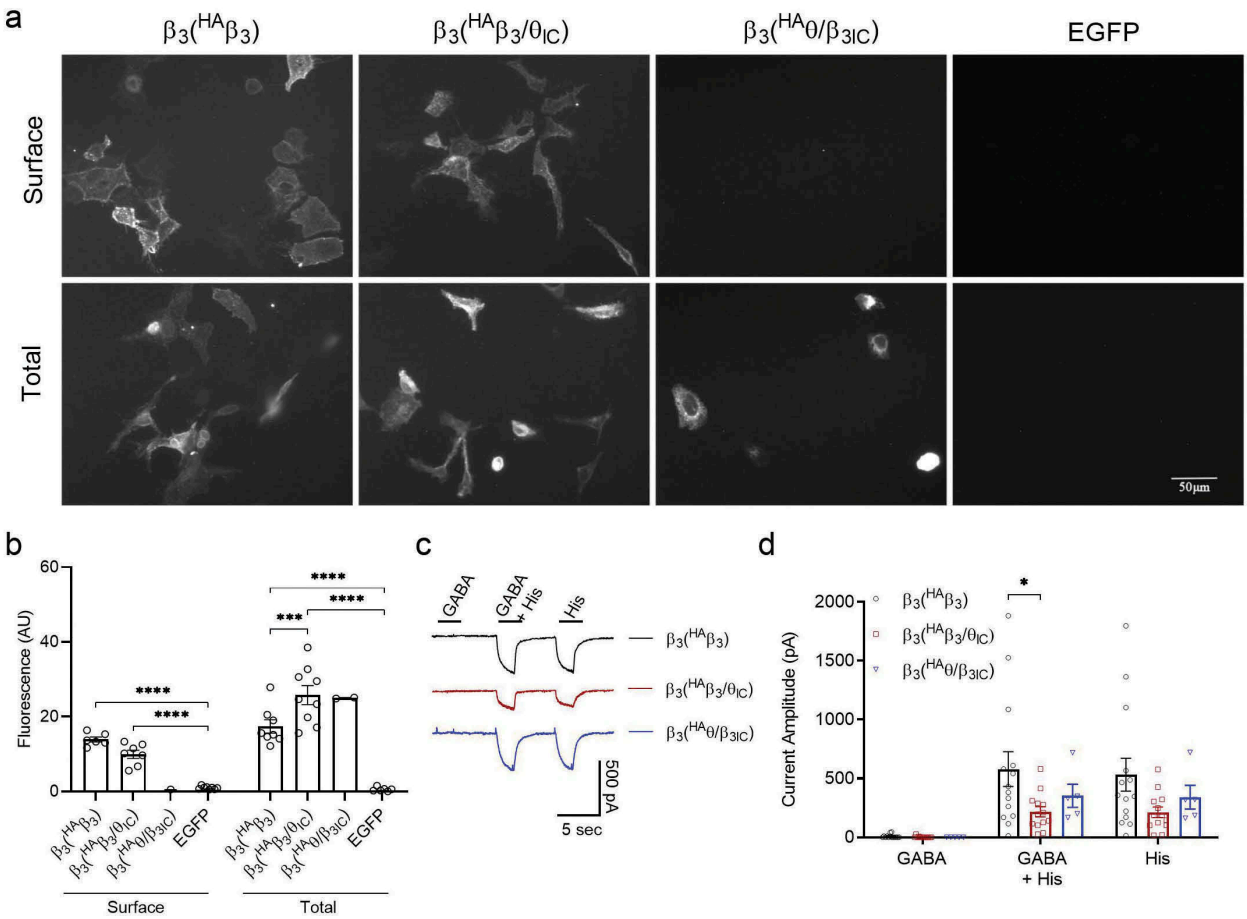

Figure 4. Pseudo-homomeric expression and function of wild type and chimeric β_3.
a) IF images at 20x magnification of non-permeabilized (surface) and permeabilized (total) staining of $^{HA}\beta_3$, $^{HA}\beta_3/\theta_{IC}$, or $^{HA}\theta/\beta_{3IC}$ in combination with β_3 co-expressed in HEK293 cells using EGFP as a negative control. Expression was determined using a rabbit anti-HA-549 antibody at 1:1000 dilution. b) Bar graphs portray the mean ± SEM of Fiji ImageJ fluorescence quantification of $\beta_3(^{HA}\beta_3)$ (n_{surf} = 6 images (49 cells), n_{total} = 8 images (67 cells)); $\beta_3(^{HA}\beta_3/\theta_{IC})$ (n_{surf} = 7 images (52 cells), n_{total} = 9 images (79 cells)); and $\beta_3(^{HA}\theta/\beta_{3IC})$ (n_{surf} = 2 images (0 cells), n_{total} = 2 images (7 cells)) IF images from a with individual data points overlaid. c) Representative traces of $\beta_3(^{HA}\beta_3)$ (n = 14), $\beta_3(^{HA}\beta_3/\theta_{IC})$ (n = 13/15), and $\beta_3(^{HA}\theta/\beta_{3IC})$ (n = 5) in response to 1 mM GABA and 3 mM histamine applied separately or together. d) Bar graphs portray the mean ± SEM of peak current amplitudes from whole-cell recordings in c with individual data points overlaid. * = $p < 0.05$; ** = $p < 0.01$; *** = $p < 0.001$; **** = $p < 0.0001$; using 2-way ANOVAs with Bonferroni post hoc comparisons.

n = 13/15; and $\beta_3(^{HA}\theta/\beta_{3IC})$ = 0 ± 0 pA, n = 5) and much larger currents evoked by 3 mM histamine ($\beta_3(^{HA}\beta_3)$ = 533 ± 123 pA, n = 14; $\beta_3(^{HA}\beta_3/\theta_{IC})$ = 213 ± 43 pA, n = 13/15; and $\beta_3(^{HA}\theta/\beta_{3IC})$ = 342 ± 90 pA, n = 5). There were no significant differences in the GABA or histamine responses for the three conditions, however the histamine-evoked current from $\beta_3(^{HA}\beta_3/\theta_{IC})$ trended toward a decrease compared to $\beta_3(^{HA}\beta_3)$ (p = 0.08). The currents elicited by GABA + histamine together were significantly different between the $\beta_3(^{HA}\beta_3)$ and $\beta_3(^{HA}\beta_3/\theta_{IC})$ conditions (580 ± 129 pA, n = 14 and 220 ± 42 pA, n = 13/15, respectively, p = 0.03) while the currents from $\beta_3(^{HA}\theta/\beta_{3IC})$ were not significantly different from either $\beta_3(^{HA}\beta_3)$ or $\beta_3(^{HA}\beta_3/\theta_{IC})$ currents ($\beta_3(^{HA}\theta/\beta_{3IC})$ = 353 ± 88 pA, n = 5). Taken together, the immunofluorescence and whole cell recordings suggest that the β_3/θ_{IC} chimera is, indeed, surface-expressed in a functional complex with wild-type β_3. However, the $^{HA}\theta/\beta_{3IC}$ chimera also gave histamine-evoked currents but no surface immunofluorescence, so we must also consider whether the functional responses are mostly or entirely generated by the wild-type subunits.

A functional tag that could distinguish the contributions of the individual subunits to overall receptor function was required to answer this question. We took advantage of a mutant β_3 subunit, $^{z}\beta_3$Q64E, which has a 50-fold higher affinity for histamine

[11] and compared the histamine potencies at $^{z}\beta_3$ Q64E homomeric receptors and pseudo-homomeric receptors containing the $^{z}\beta_3$Q64E mutant co-expressed with either $^{HA}\beta_3$, $^{HA}\beta_3/\theta_{IC}$, or $^{HA}\theta/\beta_{3IC}$ in parallel cultures of HEK293 cells. Concentration-response curves were constructed from whole cell current amplitudes evoked sequentially by increasing concentrations of histamine (from 10 μM to 10 mM), as shown in Figure 5. If the θ ICD-containing chimera is, in fact, a component of the functional surface receptor population in complex with the $^{z}\beta_3$Q64E mutant, it would cause a rightward-shift in the concentration-response and the emergence of a biphasic curve because the chimera does not carry the high-affinity mutations. If it is not, then the functional receptors should behave like $^{z}\beta_3$Q64E mutant homomers, having apparent high affinity for histamine and only one phase in the curve.

We first looked at non-permeabilized anti-HA staining to confirm that $^{z}\beta_3$Q64E could traffic with $^{HA}\beta_3$ and $^{HA}\beta_3/\theta_{IC}$ to the surface like the wild-type α_3 and β_3 subunits before. Indeed, the HA-immunofluorescence surface staining showed cells labeled in both the $^{z}\beta_3$Q64E($^{HA}\beta_3$) and the $^{z}\beta_3$Q64E($^{HA}\beta_3/\theta_{IC}$) conditions Figure 5(a,b). Like the previous α and β combinations, the surface fluorescence intensity of cells expressing $^{HA}\beta_3/\theta_{IC}$ was not significantly different compared to that of cells expressing $^{HA}\beta_3$ ($^{z}\beta_3$Q64E($^{HA}\beta_3/\theta_{IC}$) = 7.8 ± 0.8 AU, n = 9 images (26 cells); $^{z}\beta_3$Q64E($^{HA}\beta_3$) = 13.3 ± 1.9 AU, n = 11 images (46 cells)). Unsurprisingly, $^{z}\beta_3$Q64E($^{HA}\theta/\beta_{3IC}$) showed no

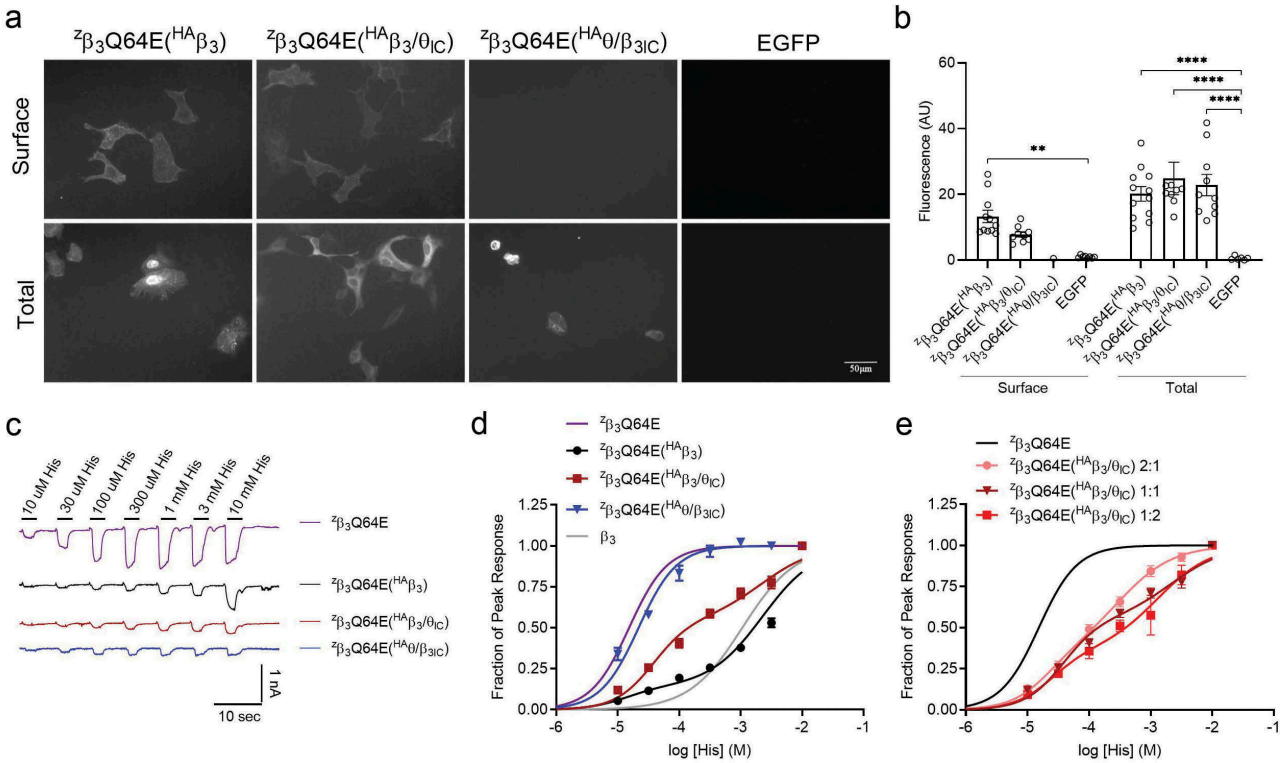

Figure 5. Histamine dose-response curves of pseudo-homomeric combinations.
a) IF images at 20x magnification of non-permeabilized (surface) and permeabilized (total) staining of $^{HA}\beta_3$, $^{HA}\beta_3/\theta_{IC}$, or $^{HA}\theta/\beta_{3IC}$ in combination with $^{z}\beta_3$Q64E co-expressed in HEK293 cells using EGFP as a negative control. Expression was determined using a rabbit anti-HA-549 antibody at 1:1000 dilution. b) Bar graphs portray the mean ± SEM of Fiji ImageJ fluorescence quantification of $^{z}\beta_3$Q64E ($^{HA}\beta_3$) (n_{surf} = 11 images (46 cells), n_{total} = 12 images (65 cells)); $^{z}\beta_3$Q64E($^{HA}\beta_3/\theta_{IC}$) (n_{surf} = 9 images (26 cells), n_{total} = 9 images (51 cells)); and $^{z}\beta_3$Q64E($^{HA}\theta/\beta_{3IC}$) (n_{surf} = 3 images (0 cells), n_{total} = 10 images (74 cells)) IF images from a with individual data points overlaid. c) Representative traces of $^{z}\beta_3$Q64E (n = 8), $^{z}\beta_3$Q64E($^{HA}\beta_3$) (n = 12), $^{z}\beta_3$Q64E($^{HA}\beta_3/\theta_{IC}$) (n = 12), and $^{z}\beta_3$Q64E($^{HA}\theta/\beta_{3IC}$) (n = 3) in response to increasing histamine concentrations from 10 μM to 10 mM. d) Normalized peak amplitudes from c plotted as a function of histamine concentration. Fit parameters: $^{z}\beta_3$Q64E EC_{50} = 15 μM; $^{z}\beta_3$Q64E($^{HA}\beta_3$) $EC_{50}1$ = 29 μM, $EC_{50}2$ = 2.4 mM; $^{z}\beta_3$Q64E($^{HA}\beta_3/\theta_{IC}$) $EC_{50}1$ = 39 μM, $EC_{50}2$ = 1.3 mM; $^{z}\beta_3$Q64E($^{HA}\theta/\beta_{3IC}$) EC_{50} = 22 μM; $^{HA}\beta_3$ EC_{50} = 1.1 mM (n = 4–8 cells per concentration). e) Normalized peak amplitudes from combinations in C using varied cDNA ratios plotted as a function of histamine concentration. Fit parameters: $^{z}\beta_3$Q64E($^{HA}\beta_3/\theta_{IC}$) 2:1 ratio $EC_{50}1$ = 21 μM, $EC_{50}2$ = 330 μM (n = 7); $^{z}\beta_3$Q64E($^{HA}\beta_3/\theta_{IC}$) 1:2 ratio EC_{50} 1 = 25 μM, $EC_{50}2$ = 1.3 mM (n = 6).

anti-HA surface labeling (n = 3 images (0 cells)). Permeabilized staining revealed similar numbers and fluorescence intensity of labeled cells ($^{z}\beta_3$ Q64E($^{HA}\beta_3$) = 20.2 ± 2.2 AU, n = 12 images (65 cells); $^{z}\beta_3$Q64E($^{HA}\beta_3/\theta_{IC}$) = 24.8 ± 4.9 AU, n = 9 images (51 cells); and $^{z}\beta_3$Q64E($^{HA}\theta/\beta_{3IC}$) = 22.8 ± 3.6 AU, n = 8 images (74 cells)).

Figure 5 also shows that the concentration-response curves were right-shifted for both $^{z}\beta_3$Q64E ($^{HA}\beta_3$) and $^{z}\beta_3$Q64E($^{HA}\beta_3/\theta_{IC}$) pseudo-homomeric combinations compared to $^{z}\beta_3$Q64E alone, while the curve for $^{z}\beta_3$Q64E($^{HA}\theta/\beta_{3IC}$) was not different from that of $^{z}\beta_3$Q64E alone Figure 5(d). As shown previously in Hoerbelt et. al. (2016)[11], $^{z}\beta_3$Q64E homomeric receptors have a very low Histamine EC_{50} (15 μM, n = 8) compared to the wild type β_3 (1.1 mM, n = 4–8 cells per concentration). Comparing the maximal peak amplitudes evoked by 10 mM histamine, the whole cell currents from $^{z}\beta_3$ Q64E($^{HA}\beta_3/\theta_{IC}$) and $^{z}\beta_3$Q64E($^{HA}\theta/\beta_{3IC}$) pseudo-homomeric receptors (275 ± 55 pA, n = 12 and 178 ± 36 pA, n = 3, respectively) were smaller than either $^{z}\beta_3$Q64E homomers (649 ± 201 pA, n = 8, $p < 0.05$) or the $^{z}\beta_3$Q64E($^{HA}\beta_3$) combination (804 ± 230 pA, n = 12, $p < 0.05$). Moreover, the concentration-response curves for the $^{z}\beta_3$Q64E($^{HA}\beta_3$) and the $^{z}\beta_3$Q64E($^{HA}\beta_3/\theta_{IC}$) combinations were clearly bimodal, having two components with markedly different concentration dependence. The histamine EC_{50} for homomeric $^{z}\beta_3$Q64E was 15 μM (n = 8), which was similar to $^{z}\beta_3$Q64E($^{HA}\theta/\beta_{3IC}$) (22 μM, n = 3) and the high-affinity component in both $^{z}\beta_3$Q64E($^{HA}\beta_3$) heteromers (16 μM, n = 12) and $^{z}\beta_3$Q64E($^{HA}\beta_3/\theta_{IC}$) heteromers (29 μM, n = 12). The low-affinity component for the for $^{z}\beta_3$Q64E($^{HA}\beta_3$) curve had an EC_{50} of 2.4 mM (n = 12) and represented 85% of the total curve fit, while the low-affinity component for the $^{z}\beta_3$ Q64E($^{HA}\beta_3/\theta_{IC}$) curve had an EC_{50} of 1.3 mM (n = 8) and represented 53% of the total curve fit. These results confirm that the $^{HA}\beta_3/\theta_{IC}$ chimera indeed assembles with other β_3 subunits and contributes to the functional response, but to a slightly lesser extent than wild-type $^{HA}\beta_3$ while the $^{HA}\theta/\beta_{3IC}$ chimera remains ER retained.

Figure 5(e) explores the effect of subunit ratios on shifting the concentration-response curve toward the high-affinity or low-affinity phenotypes. To this end, we compared $^{z}\beta_3$Q64E($^{HA}\beta_3/\theta_{IC}$) at 2:1, 1:1, and 1:2 ratios of cDNA. The maximal peak amplitudes evoked by 10 mM histamine were 754 ± 278 (n = 7), 275 ± 58 pA (n = 12), and 114 ± 22 pA (n = 6), respectively, consistent with a reduction in total surface receptors as the number of β ICDs was reduced. Regardless of the subunit ratio, the concentration-response curves retained their bimodality, suggesting that the HA-tagged constructs were assembled with the $^{z}\beta_3$Q64E construct. The high-affinity component of the $^{z}\beta_3$Q64E($^{HA}\beta_3/\theta_{IC}$) curves at 2:1, 1:1, and 1:2 ratios had an EC_{50} of 21 μM (n = 7), 29 μM (n = 12), and 25 μM (n = 6), respectively, which are all comparable to the EC_{50} for $^{z}\beta_3$Q64E (15 μM, n = 8). Similarly, the low-affinity component of the $^{z}\beta_3$ Q64E($^{HA}\beta_3/\theta_{IC}$) curves at 1:2 and 1:1 ratios both had an EC_{50} of 1.3 mM (1:2 ratio n = 6, 1:1 ratio n = 12) which is comparable to the EC_{50} for wild-type β_3 (1.1 mM, n = 4–8 cells per concentration). The low-affinity component accounted for 64% of the $^{z}\beta_3$Q64E($^{HA}\beta_3/\theta_{IC}$) curve at 1:2 ratio compared to 53% at 1:1. Interestingly, the low-affinity component was also 64% of the curve fit for $^{z}\beta_3$Q64E($^{HA}\beta_3/\theta_{IC}$) at 2:1 ratio, but the fit had an EC_{50} of 330 μM (n = 7), suggesting a difference in the number or functional impact of low-affinity sites present at the surface in this condition. The inverse relationship between maximal current amplitudes and the $^{HA}\beta_3/\theta_{IC}$ content implies that multiple copies of the β_3 ICD are probably required in the pentamer to overcome ER retention and traffic the receptor to the surface.

Discussion

$GABA_A$ receptors are functionally expressed on the cell surface. This requires translation by ER-associated ribosomes, the proper folding of the individual subunit proteins, their assembly into pentameric ion channels, and their trafficking through the secretory pathway to the plasma membrane where they can respond to extracellular signals. The cellular mechanisms that regulate folding, assembly and trafficking are not completely understood. Some of the more general maturation processes involve common ER chaperones like calnexin, BiP, and protein disulfide isomerase, which aid in folding, glycosylation, and formation of intra- or inter-subunit disulfide bonds [12]. Others may be more specific for particular subunits or combinations of subunits. Which subunits are compatible to assemble with one another, for

example, appears to be determined by their extracellular ligand binding loops A-E and the GKER motif in loop F of the NTD [3,7,12]. Then, trafficking of the pentameric receptors from ER to the plasma membrane might occur by default but often appears to involve cytosolic chaperone proteins that interact with the cytoplasmic TM3-TM4 loops of different subunits to help guide and cluster the receptors to the appropriate location on the plasma membrane [13,14].

In the present study, we sought to test whether and how the ICD is involved in β_3 homomeric and heteromeric functional expression. The β_3 subunit can form homo-pentameric ion channels, unlike β_2, and previous studies suggested this could be fully explained by differences in an "assembly motif" (GKER/DNTK) in Loop F of their NTD binding domains [7]. Up to now, the β ICD was not known to regulate recombinant functional expression. To explore the role of the ICD, we created reciprocal chimeric exchanges of the TM3-TM4 ICD between the β_3 and θ subunits. We expected that the θ ICD would support the functional expression of chimeric β_3/θ homomers. It did not. While the θ ICD did not disrupt assembly, our data revealed that the θ ICD could not support ER export and trafficking of receptors unless it was co-assembled with α or β subunits bearing their natural ICD. Of note, it is curious that the $^{HA}\theta/\beta_{3IC}$ chimera was not surface expressed in combination with α as previously reported for the wild-type θ subunit[9], but our data suggest they fail to co-assemble.

Results show that $^{HA}\beta_3$ homomeric receptors can traffic to the plasma membrane while neither the $^{HA}\beta_3/\theta_{IC}$ chimera nor the $^{HA}\theta/\beta_{3IC}$ chimera could do this. By contrast, we also show that pseudo-homomeric receptors composed of the $^{HA}\beta_3/\theta_{IC}$ chimera plus wild-type β_3 or the high-affinity $^{z}\beta_3$ mutant are functionally expressed on the plasma membrane, as are heteromeric receptors composed of the $^{HA}\beta_3/\theta_{IC}$ chimera plus wild-type α_3. Taken together, three conclusions can be drawn from these results: (1) the β_3 ICD is necessary for functional expression of the homomeric receptor, (2) the α_3 ICD likewise promotes functional expression of the heteromeric receptor, and (3) the θ ICD contains neither permissive signals to promote surface expression nor inhibitory signals to prevent it. In the rare cases where homomeric $^{HA}\beta_3/\theta_{IC}$ was seen to reach the plasma membrane, these too may be pseudo-homomers assembled with endogenous β_3, which is expressed in HEK293 cell cultures at low levels in the culture [15] as a whole, or involve some other factor that varies from cell to cell and leads to a few positively stained cells. Based on the absence of $^{HA}\theta/\beta_{3IC}$ surface staining under any conditions, and the fact that θ does not assemble as a homomeric receptor [9], we can also conclude that the β_3 ICD is not sufficient to drive surface expression if the subunits are not assembled. Although this study did not test other subunit ICDs, we propose that $\beta_{1\text{-}3}$ all contain similar anterograde trafficking signals. This is supported by previous reports by other groups showing that homomeric β_1 expression[3], and homomeric β_2 mutants having the assembly-permissive GKER motif in their F-loop but still having the β_2 ICD were also functionally expressed[7].

Virtually all neurons in the CNS express functional $GABA_A$ receptors. Some of the 19 available subunits (e.g., α_1, $\beta_{2\text{-}3}$,γ_2) are expressed abundantly throughout the brain and are well characterized in native and recombinant systems[1]. Others are far less common (e.g., γ_1, γ_3, θ, ε, π) and are poorly understood[1]. Heterologous expression systems are often used in combination with mutagenesis to foster understanding of which subunits or combinations of subunits are functionally expressed, how they work and how they are regulated. HEK293 cells are by far the most commonly used mammalian cell line for the study of ligand-gated ion channels (LGIC), including $GABA_A$ receptors, because they do not express LGIC subunits in an amount that would confound interpretation [15]. They are considered, in this regard, to be a blank slate. It is important, however, to consider that HEK293 cells are not neurons and, just as they generally do not express neuronal receptors, they also might not express all the proper machinery to process or traffic neuronal receptors in the same manner as neurons. This may be especially true for receptors or other cargo destined to axonal/presynaptic compartments, which HEK293 cells do not have.

Recent studies have made this point clearly with respect to nicotinic acetylcholine receptors (nAChR). The most widely expressed neuronal

nAChRs, the α7 and $\alpha4\beta_2$ subtypes, have been notoriously difficult to study in mammalian cell lines because they are not functionally expressed [16–19]. However, co-expression of the putative chaperone/accessory proteins RIC-3 or TMEM35A/NACHO can permit robust functional expression of these nAChRs in HEK293 cells [17–21].

Our data indicate the $^{HA}\beta_3/\theta_{IC}$ chimera alone rarely reaches the plasma membrane, whereas co-expression with either wild-type α_3 or β_3 rescues its surface expression. The defect in $^{HA}\beta_3/\theta_{IC}$ homomeric expression appears to reflect a trafficking error, not an assembly error, because the pseudo-homomeric $^{HA}\beta_3/\theta_{IC}$ plus wild-type β_3 receptors are functionally expressed. From this we can infer that α_3 and β_3 subunits both contain anterograde trafficking signals that can overcome ER retention of the assembled receptors. In $GABA_A$ subunits, and across all subunits of the pentameric ion channel superfamily, the TM3-TM4 intracellular loop is the most variable region both in terms of length and amino acid composition.

A number of cytosolic chaperones have been proposed to regulate $GABA_A$ receptor trafficking by interactions involving the ICD of α, β or γ subunits. The first and best characterized chaperone shown to be involved in $GABA_A$ receptor trafficking is the $GABA_A$ receptor-associated protein, or GABARAP [22]. GABARAP acts by interacting with the γ_2 ICD to promote plasma membrane expression [23]. Other cytosolic chaperones such as BIG2 (brefeldin A-inhibited GDP/GTP exchange factor 2), NSF (N-ethylmaleimide-sensitive factor), and PRIP1 (PLC-related catalytically inactive protein 1) all interact with the ICD of $\beta_{1\text{-}3}$ [24–27]. Gephryn and PLIC1 (protein linking integrin-associated protein to cytoskeleton-1) interact with both α and β ICDs [14,28]. Except for PRIP1, these chaperone proteins and others are expressed at moderate to high levels in HEK293 cells (GEO accession number GDS5213) [29]. It remains to be determined how these proteins interact with the ICDs and which, if any, are required for functional expression of various subtypes of $GABA_A$ receptors in HEK293 cells.

It is perhaps worth noting the relative homology among the synaptically expressed α, β, γ subunits, which are all readily expressed in heterologous systems. The rat β1-3 ICDs share 48–54% amino acid sequence identity, while the α1-3 and α5 ICDs are 36–62% identical, and the γ1-3 ICDs are 52–56% identical by comparing BLAST alignments. In contrast, the θ ICD has no homology in the rat genome and the non-synaptic α4, α6 and δ ICDs are likewise each unique. So, one question raised from this study remains: why do $GABA_A$ β homomers and αβ heteromers express in HEK293 cells but the β/θ_{IC} chimera does not? If certain nAChRs are a precedent, it may be that the θ ICD requires interactions with a unique chaperone protein found only where θ is naturally expressed. If so, the β/θ_{IC} chimera could well express in another system, for example in neurons, or in heterologous cells upon co-expression of appropriate chaperones that are yet to be identified. Trafficking might also be amenable to proteostatic enhancement by small molecules [30]. As a whole, this study shows the involvement of the ICD in β_3 homomeric and heteromeric functional expression and raises questions about the ICD of less common $GABA_A$ subunits, such as θ. Further work is needed to determine precisely where the critical ICD motifs reside and to understand how the assembly and trafficking of β, θ, and the β/θ chimeric subunits are functionally regulated.

Methods

Drugs and solutions

Recording solution components, buffer components, GABA (cat. #A2129), histamine dihydrochloride (cat. #H7250) were purchased from Sigma-Aldrich (St. Louis, MO). GABA was dissolved in extracellular recording solution at a 1 M stock concentration, then stored at 4°C. Histamine was dissolved at a 30 mM stock concentration and the pH was adjusted to neutral. This stock histamine solution was made freshly or stored at −20°C for up to 72 hr. Stock drug solutions were diluted on the day of the experiment. Concentration-response curve solutions were made by serial dilution.

cDNA and mutagenesis

All cDNA constructs were expressed in the pRK5 vector carrying the CMV promoter and ampicillin-resistance. Subcloning-efficiency E. coli were

used as the host for cDNA copy replication. Rat α_3 (accession no. L08492.1) and β_3 (X15468.1) subunit cDNAs in the pRK5 vector were given generously by Dr. Peter Seeburg (Max Planck Institute for Medical Research, Heidelberg, Germany). Rat θ (AF419333.1) subunit cDNA was generously provided by Dr. Maurice Garrett (University of Bordeaux, Bordeaux, France) in the pcDNA3 vector and transferred into the pRK5 vector between BamHI (5′) and XbaI (3′) upon receipt. The coding region and UTRs were confirmed by Sanger sequencing for all subunit cDNAs and subsequent mutations. We identified two separate point mutations (causing H362N and L400M) within the ICD of our θ cDNA and one point mutation causing S296T in the third TMD of α_3 that differ from the published sequences.

$^{HA}\beta_3$, $^{HA}\theta$, $^{HA}\beta_3/\theta_{IC}$, and $^{HA}\theta/\beta_{3IC}$ were all created using *NEBuilder HiFi DNA assembly kit* (New England Biolab, Ipswich, MA, E5520S). The hemagglutinin tag was a triplet of HA epitopes flanked by AgeI (5′) and NotI (3′) endonuclease sites. PCR primers were designed using the NEBuilder Assembly Tool v1.12. To make $^{HA}\beta_3$, the triplet HA tag, TGLD**YPYDVPDYA**G**YPYD VPDYA**GS**YPYDVPDYA**AAA, was inserted between amino acids 6 and 7 of the mature β_3 protein using the manufacturer's protocol. In short, PCR was used to isolate and amplify the fragments of interest (linearized β_3 and the HA tag). The fragments were then assembled by mixing and incubating at 50°C with the NEBuilder HiFi DNA Assembly Master Mix for ≥ 15min. The assembled product was then transformed into NEB5α competent cells and spread onto ampicillin-resistant plates, clonal colonies were picked and screened by endonuclease digestion. The $^{HA}\theta$/pRK5 construct was made in the same manner as $^{HA}\beta_3$/pRK5 except that the HA tag was inserted between amino acids 5 and 6 of the mature protein.

The $^{HA}\beta_3/\theta_{IC}$ construct was made by linearizing $^{HA}\beta_3$/pRK5 without the M3-M4 loop (IVFPFT … YIFFGR) and isolating the θ M3-M4 loop (RNHRRC … VPKVDR) from $^{HA}\theta$/pRK5 using PCR. Likewise, to make the $^{HA}\theta/\beta_{3IC}$ construct, $^{HA}\theta$/pRK5 was linearized (LFPLSF … YLFFSQ) and the β_3 M3-M4 loop (QRQKKL … AIDRWS) was isolated from $^{HA}\beta_3$/pRK5 using PCR. Fragments for both chimeras were then assembled and screened in the same manner as above.

The $^{z}\beta_3$Q64E construct was made previously and described in Hoerbelt et. al. (2016).

Cell culture and transfections

HEK293 cells (ATCC CRL-1573) were cultured at 37°C with 5% CO2 in Minimal Essential Medium plus glutamine (MEM, Gibco, Gaithersburg, MD) with 10% fetal bovine serum (Gibco) and 5% Penicillin-Streptomycin (Gibco) added. For immunofluorescence experiments and electrophysiological recording, cells were plated at 100,000/dish in Poly-D-Lysine (Sigma-Aldrich) coated 6-well plates (Corning) or 35 mm Nunc dishes (Nalge Nunc, Naperville, IL), left overnight to adhere, and then transfected with a total of the following per dish/well: 1 μg total cDNA (subunit ratios of 1:1 for co-transfections, unless otherwise stated), 0.82 μL Lipofectamine 2000 (Invitrogen), and 100 μL total serum-free MEM. Components were mixed using the manufacturer's protocol. 100 μL of the transfection mixture was dripped in an outward spiraling motion into each dish or well. For Western blotting experiments, non-coated 60 mm dishes were used and cell density and transfection volumes were scaled up by a ratio of 0.4 due to the increase in surface area of the dish. Cells were used 36–40 hr post-transfection for immunofluorescence and Western blotting experiments and 20–48 hr post-transfection for electrophysiological recording. For electrophysiology transfections, EGFP/pRK5 was co-transfected with the $GABA_A$ subunits as 10% of the total cDNA, and only cells expressing the EGFP were targeted to patch.

Western blot

At 36–40h post transfection, HEK293 cells plated in 60 mm dishes were washed twice by PBS then lysed in 2% SDS + 8 mM EDTA. A fraction of the lysates was saved for a BCA analysis while the remaining fraction of the lysates was diluted 1:1 with reducing Laemmeli buffer (with 5% β-Mercaptoethanol). 10–20 μg of total protein was separated using a 10% SDS-PAGE gel. Separated proteins were

then transferred to a nitrocellulose membrane. The membranes were washed with tris-buffered saline (pH = 7.4) + 0.1% Tween-20 (TBST) and then blocked with 5% milk in TBST. Blocked membranes were incubated at 4°C overnight in primary rabbit anti-HA Epitope Tag (1 mg/ml, diluted 1:5000 in 5% milk + TBST, Rockland Antibodies & Assays cat. #600-401-384). After washing thoroughly, the membranes were probed with secondary HRP-conjugated goat anti-rabbit IgG (1 mg/ml, diluted 1:5000 in 5% milk + TBST, Invitrogen cat. #ABIN964977) for 1 h at room temperature. Immunoreactivity was visualized using Pierce™ ECL Western Blotting Substrate (ThermoFisher Scientific cat. #32,106) in a ChemiDoc Imaging System (BioRad, Hercules, CA, USA). Membranes were then incubated with primary rabbit anti-GAPDH (1 mg/ml, diluted 1:5000 in 5% milk + TBST, Sigma-Aldrich #G9545) for 1 h at room temperature. After washing well, the membranes were probed with the same secondary and visualized again as above. Band intensities and molecular weights were quantified using the ImageJ (NIH) gel analysis tool[31]. Blot images were post processed on a personal computer using Photoshop software for presentation.

Immunofluorescence (IF)

At 36–40h post transfection, HEK293 cells plated in 6-well plates were washed in sucrose solution (290 mM sucrose, 5 mM HEPES, 3 mM KCl, 1.8 mM $CaCl_2$, and 1 mM $MgCl_2$; pH 7.3), then cells were washed in tris-buffered saline (TBS, pH 7.4), and fixed in TBS + 3.7% formaldehyde (pH 7.4). After fixation, cells were washed in TBS, blocked in TBS + 5% goat serum, then incubated for 1 hr in rabbit anti-HA Epitope Tag DyLight™ 549 conjugated antibody (1 mg/ml, diluted 1:1000 in TBS + 5% goat serum, Rockland Antibodies & Assays #600-442-384). After washing with TBS, cells were visualized on an Olympus IX71 fluorescence microscope fitted with a LUCPlanFl 20X/0.4 RC2 (∞/) objective. Non-permeabilized fluorescent photomicrographs were captured at the same exposure with a QImaging QICAM digital camera (1X). After capturing non-permeabilized photomicrographs, the cells were then permeabilized in TBS + 0.1% TritonX-100. After permeabilization, cells were washed with TBS, blocked in TBS + 5% goat serum, re-incubated for 1 hr in the same antibody as above, and washed again with TBS. Cells were then visualized, and fluorescent photomicrographs of permeabilized staining were captured, as above. Both non-permeabilized (surface) and permeabilized (total) photomicrographs were post processed on a personal computer using Photoshop software for presentation.

Immunofluorescence quantification

Average fluorescent intensities were calculated using Fiji ImageJ [31,32]. Using the 192 immunofluorescence photomicrographs captured as above, the fluorescent cells were manually outlined in each image, then the average fluorescent intensity was calculated and the background fluorescence was subtracted. The fluorescent intensities of immune-positive cells were reported in arbitrary units (AU).

Electrophysiological recordings

Whole-cell patch clamp was used to examine the function of $GABA_A$ receptors as in Fleck (2002) and Hoerbelt et al. (2015). Briefly, at 20–48 hr post-transfection HEK293 cells were superfused with extracellular recording solution (pH 7.3–7.4; 295–305 mOsm) consisting of 0.1 mg/ml phenol red pH indicator and (in mM): 145 NaCl, 5 HEPES, 3 KCl, 1.8 $CaCl_2$ and 1 $MgCl_2$. Thin-walled borosilicate glass microelectrodes were 3–7MΩ when filled with intracellular recording solution (pH 7.3; 295–305 mOsm) consisting of (in mM): 135 CsCl, 10 CsF, 10 HEPES, 5 EGTA, 1 MgCl2 and 0.5 $CaCl_2$. Patch recordings were conducted in voltage-clamp mode at −80 mV, causing inward chloride currents with V_{rev} around 0 mV under these ionic conditions. Current signals were recorded and analyzed on a Macintosh computer using Synapse software (Synergistic Research Systems, Silver Spring, MD). Drugs were applied mostly as described in Fleck (2002) and Hoerbelt et al. (2015). Briefly, 4 or 8 syringes were loaded with extracellular recording solution with and without GABA and/or histamine and driven at 1.5 ml/min through a single glass flow-pipe combining these 4 or 8 barrels. The flow pipe had a ~200 mm diameter tip and was placed <1 mm from the target

cell to allow complete superfusion of the cell. Rapid solution exchange (5–20ms) was provided by 3-way solenoid valves (Lee Co., Westbrook, CT) controlled by the computer. The protocols used for drug application were consistently 2 sec drug application pulses with at least 5 sec control solution application between each drug pulse.

Data analysis and statistics

Current traces were analyzed with Synapse software (Silver Spring, MD), Kaleidagraph (Synergy Software, Reading, PA), GraphPad Prism 8 (San Diego, CA), and Microsoft Excel. All comparisons were made using cells transfected in parallel and recording dishes were alternated by transfection subtype. Current amplitudes were measured from baseline to peak, where the baseline was taken during control period immediately before the switch to drug application. Cells with noisy or unstable baselines were excluded from analysis. Histamine potentiation was assessed by comparing the current amplitude during combined application of GABA + histamine (or the extent of potentiation) to the current amplitude of the initial pulse of GABA alone. Concentration response curves were fit using the following equation:

$$I_{[agonist]} = \frac{I_{max}}{1 + \left(\frac{EC_{50}}{[agonist]}\right)^{n_H}}$$

Where I_{max} = maximum current, EC_{50} = concentration at half maximal current, and n_H = Hill coefficient. Current amplitudes for concentration response curves were normalized to the highest concentration of agonist tested then averaged. Biphasic histamine concentration response curves were fit using the following equation:

$$I_{[agonist]} = \frac{I_{HA}}{1 + \left(\frac{EC_{50}1}{[agonist]}\right)^{n_{H1}}} + \frac{100 - I_{HA}}{1 + \left(\frac{EC_{50}2}{[agonist]}\right)^{n_{H2}}}$$

Where I_{HA} = maximum high affinity current, n_{H1} = Hill coefficient of the high affinity component (constrained to 1.4 based on the control fit to $^{z}\beta_3$ Q64E), $EC_{50}1$ = concentration at half maximal current of the high affinity component, n_{H2} = Hill coefficient of the low affinity component (constrained to 1.0 based on the control fit to wild type β_3), and $EC_{50}2$ = concentration at half maximal current of the low affinity component. Notably, there is a ~3 mV drop in Cl^- driving force at the highest histamine concentration tested (10 mM histamine dihydrochloride) which was not compensated. Half maximal (EC_{50}) values from multiple replicates per group are presented as the mean ± the 95% confidence interval. Other data are shown as mean ± SEM and n values refer to either the number of images analyzed followed by the total number of cells in all images acquired in parentheses or the number of cells recorded. For all statistical comparisons, a p value < 0.05 is considered statistically significant.

Acknowledgments

We are grateful to Maurice Garret and Peter Seeburg for the $GABA_A$ cDNAs and Ellinor Grinde for her technical assistance.

Author contributions

Both authors wrote and revised the main manuscript and JN prepared the figures.

Disclosure statement

No potential conflict of interest was reported by the authors.

Funding

This work was supported by Albany Medical College.

Data availability

All data generated or analyzed during this study are included in this published article. Datasets analyzed are available from NCBI, accession number GDS5213.

References

[1] Olsen RW, Sieghart W. International union of pharmacology. LXX. Subtypes of gamma-aminobutyric acid(A) receptors: classification on the basis of subunit composition, pharmacology, and function. Update. Pharmacol Rev. 2008;60:243–260.
[2] Smith GB, Olsen RW. Functional domains of GABAA receptors. Trends Pharmacol Sci. 1995;16:162–168.
[3] Bollan K, Robertson LA, Tang H, et al. Multiple assembly signals in gamma-aminobutyric acid (type A)

receptor subunits combine to drive receptor construction and composition. Biochem Soc Trans. 2003;31:875–879.
[4] Ehya N, Sarto I, Wabnegger L, et al. Identification of an amino acid sequence within GABA(A) receptor beta3 subunits that is important for receptor assembly. J Neurochem. 2003;84:127–135.
[5] Klausberger T, Sarto I, Ehya N, et al. Alternate use of distinct intersubunit contacts controls GABAA receptor assembly and stoichiometry. J Neurosci. 2001;21:9124–9133.
[6] Taylor PM, Connolly CN, Kittler JT, et al. Identification of residues within GABA(A) receptor alpha subunits that mediate specific assembly with receptor beta subunits. J Neurosci. 2000;20:1297–1306.
[7] Taylor PM, Thomas P, Gorrie GH, et al. Identification of amino acid residues within GABA(A) receptor beta subunits that mediate both homomeric and heteromeric receptor expression. J Neurosci. 1999;19:6360–6371.
[8] Connolly CN, Krishek BJ, McDonald BJ, et al. Assembly and cell surface expression of heteromeric and homomeric gamma-aminobutyric acid type A receptors. J Biol Chem. 1996;271:89–96.
[9] Bonnert TP, McKernan RM, Farrar S, et al. Theta, a novel gamma-aminobutyric acid type a receptor subunit. Proc Natl Acad Sci Usa. 1999;96:9891–9896.
[10] Saras A, Gisselmann G, Vogt-Eisele AK, et al. Histamine action on vertebrate GABAA receptors: direct channel gating and potentiation of GABA responses. J Biol Chem. 2008;283:10470–10475.
[11] Hoerbelt P, Ramerstorfer J, Ernst M, et al. Mutagenesis and computational docking studies support the existence of a histamine binding site at the extracellular beta3 +beta3- interface of homooligomeric beta3 GABAA receptors. Neuropharmacology. 2016;108:252–263.
[12] Sarto-Jackson I, Sieghart W. Assembly of GABA(A) receptors (Review). Mol Membr Biol. 2008;25:302–310.
[13] Charych EI, Liu F, Moss SJ, et al. GABA(A) receptors and their associated proteins: implications in the etiology and treatment of schizophrenia and related disorders. Neuropharmacology. 2009;57:481–495.
[14] Tretter V, Mukherjee J, Maric H-M, et al. Gephyrin, the enigmatic organizer at GABAergic synapses. Front Cell Neurosci. 2012;6:23.
[15] Thomas P, Smart TG. HEK293 cell line: a vehicle for the expression of recombinant proteins. J Pharmacol Toxicol Methods. 2005;51:187–200.
[16] Cooper ST, Millar NS. Host cell-specific folding and assembly of the neuronal nicotinic acetylcholine receptor alpha7 subunit. J Neurochem. 1997;68:2140–2151.
[17] Koperniak TM, Garg BK, Boltax J, et al. Cell-specific effects on surface alpha7 nicotinic receptor expression revealed by over-expression and knockdown of rat RIC3 protein. J Neurochem. 2013;124:300–309.
[18] Lansdell SJ, Gee VJ, Harkness PC, et al. RIC-3 enhances functional expression of multiple nicotinic acetylcholine receptor subtypes in mammalian cells. Mol Pharmacol. 2005;68:1431–1438.
[19] Millar NS. RIC-3: a nicotinic acetylcholine receptor chaperone. Br J Pharmacol. 2008;153(Suppl 1): S177–183.
[20] Gu S, Matta JA, Lord B, et al. Brain alpha7 nicotinic acetylcholine receptor assembly requires NACHO. Neuron. 2016;89:948–955.
[21] Matta JA, Gu S, Davini WB, et al. NACHO mediates nicotinic acetylcholine receptor function throughout the brain. Cell Rep. 2017;19:688–696.
[22] Chen ZW, Chang CS, Leil TA, et al. GABAA receptor-associated protein regulates GABAA receptor cell-surface number in Xenopus laevis oocytes. Mol Pharmacol. 2005;68:152–159.
[23] Nymann-Andersen J, Wang H, Chen L, et al. Subunit specificity and interaction domain between GABA(A) receptor-associated protein (GABARAP) and GABA(A) receptors. J Neurochem. 2002;80:815–823.
[24] Charych EI, Yu W, Miralles CP, et al. The brefeldin A-inhibited GDP/GTP exchange factor 2, a protein involved in vesicular trafficking, interacts with the beta subunits of the GABA receptors. J Neurochem. 2004;90:173–189.
[25] Goto H, Terunuma M, Kanematsu T, et al. Direct interaction of N-ethylmaleimide-sensitive factor with GABA(A) receptor beta subunits. Mol Cell Neurosci. 2005;30:197–206.
[26] Kittler JT, Rostaing P, Schiavo G, et al. The subcellular distribution of GABARAP and its ability to interact with NSF suggest a role for this protein in the intracellular transport of GABA(A) receptors. Mol Cell Neurosci. 2001;18:13–25.
[27] Terunuma M, Jang I-S, Ha SH, et al. GABAA receptor phospho-dependent modulation is regulated by phospholipase C-related inactive protein type 1, a novel protein phosphatase 1 anchoring protein. J Neurosci. 2004;24:7074–7084.
[28] Bedford FK, Kittler JT, Muller E, et al. GABA(A) receptor cell surface number and subunit stability are regulated by the ubiquitin-like protein Plic-1. Nat Neurosci. 2001;4:908–916.
[29] Iwashita Y, Fukuchi N, Waki M, et al. Genome-wide repression of NF-kappaB target genes by transcription factor MIBP1 and its modulation by O-linked beta-N-acetylglucosamine (O-GlcNAc) transferase. J Biol Chem. 2012;287:9887–9900.
[30] Di XJ, Han DY, Wang YJ, et al. SAHA enhances Proteostasis of epilepsy-associated alpha1(A322D)beta2gamma2 GABA(A) receptors. Chem Biol. 2013;20:1456–1468.
[31] Schneider CA, Rasband WS, Eliceiri KW. NIH Image to ImageJ: 25 years of image analysis. Nat Methods. 2012;9:671–675.
[32] Schindelin J, Arganda-Carreras I, Frise E, et al. Fiji: an open-source platform for biological-image analysis. Nat Methods. 2012;9:676–682.